

## EFFECTS OF PARAMETER UNCERTAINTIES ON LONGITUDINAL WEB DYNAMICS

By

**Jonathan Frechard, Dominique Knittel, and Yannick Martz**  
University of Strasbourg  
FRANCE

### ABSTRACT

Web handling systems are very common in industry for metal, paper, textile and polymer material treatments. The key variables to monitor and control are the web speed and web tension in each span. The objective is to reach the expected web speed while maintaining web tension in an acceptable range around the tension reference. Nevertheless, the longitudinal web dynamic behavior is sensitive to parameter variations or parameter uncertainties, as for example the web elasticity, the web speed, the roll radius.

The implemented control strategy is a classical one: a first loop ensures roller speed control whereas the external loop ensures web tension control. The web tension controllers are automatically synthesized using an optimization approach. The influences of parameter variations are studied firstly on the open-loop system and then on the closed-loop behavior.

### NOMENCLATURE

$V_i$	Web linear speed
$T_i$	Web tension in the span $i$
$J_i$	Inertia of the roller $i$
$K_i$	
$R_i$	Radius of the roller $i$
$f_d$	Web/roller dynamic friction coefficient
$\epsilon_i$	Strain of the web span $i$
$L_i$	Length of the web span $i$
$E$	Young Modulus
$S$	Web cross-section
$u_i$	Control signal of the roller $i$

## INTRODUCTION

Roll-to-roll systems are very common in industry for metal, paper, textile and polymer material treatments. The key variables to monitor and control are the web speed and web tension in each span. The objective is to reach the expected web speed while maintaining web tension in an acceptable range around the tension reference [1]. The nonlinear and linear models of a web transport system are built from the equations describing web tension behavior between two consecutive rollers and the velocity of each roller [2, 3]. The studied plant is composed of an unwinder, two intermediate motor driven rollers, twenty-five idle rollers and a rewinder. Tension control in both unwind and rewind sections are performed by using pendulum dancers, while it is ensured by using load cells in the process section.

The speed controller can be easily calculated whereas the tension controller is more difficult to synthesize. Industry usually uses PI or PID controller for web tension control. PI or PID web tension controller can be computed, in a convenient and efficient way, in the fixed-order and fixed-structure  $H_\infty$  synthesis framework [4, 5]. Nevertheless, the dynamic performances and the stability range decrease when system parameters are varying.

This work analyses the effects of parameter uncertainties or variations on longitudinal web dynamics. The considered parameters are web elasticity, web nominal speed and wound roll radius.

Firstly, a physical nonlinear model is established for the studied plant. This model is then linearized around a setting point. The linear model enables the calculation of the optimal controllers. The influences of parameter variations on the global system performances are analyzed.

## SYSTEM MODELING

The system under study is composed of an unwinder, a rewinder, 2 pendulum dancers, 30 idle rollers, 2 motor driven rollers, several load cells. The two pendulum dancers are located close to the unwinder and rewinder (see Fig. 1, the rollers marked with the letter J are equipped with load cells).

The equations describing the dynamic behavior of web tension and velocity permit to construct the global model of the plant.

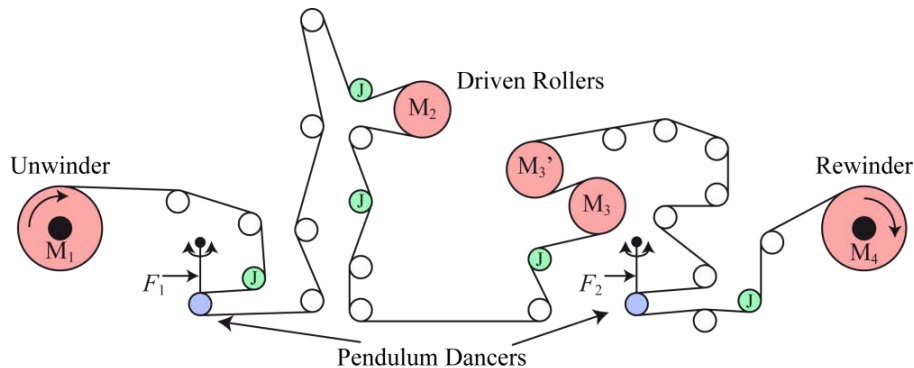


Figure 1 – Scheme of the studied plant

### Web Dynamics

Assuming that no slippage between the web and the rollers occurs, the velocity of the  $i^{\text{th}}$  roller is obtained by the application of torque balance:

$$\frac{d(J_i \Omega_i)}{dt} = R_i (T_{i-1} - T_i) + K_i U_i - C r_i \quad \{1\}$$

where  $J_i$  is the roller inertia,  $\Omega_i$  is the  $i^{\text{th}}$  roller velocity.  $T_{i-1}$  and  $T_i$  are respectively the upstream and downstream web tension.  $K_i$  is the torque gain (current loop).  $U_i$  is the control signal and  $C r_i$  is the roller friction. Of course,  $K_i U_i$  is equal to zero for idle rollers.

The web strain  $\varepsilon_i$  between two consecutive rollers depends on the rollers velocity [2]:

$$\frac{d}{dt} \left( \frac{L_i}{1 + \varepsilon_i} \right) = - \frac{V_{i+1}}{1 + \varepsilon_i} + \frac{V_i}{1 + \varepsilon_{i-1}} \quad \{2\}$$

where  $L_i$  is the web span length,  $V_{i+1}$  is the downstream roller speed,  $V_i$  is the upstream roller speed and  $\varepsilon_{i-1}$  is the upstream web strain.

The web tension  $T$  is obtained using Hooke's law:

$$T = ES\varepsilon \quad \{3\}$$

where  $E$  is the web Young's modulus and  $S$  is the web cross-section.

### Pendulum Dancer Modeling

The pendulum dancer, shown in Fig. 2 permits to indirectly control web tension in the unwinding and rewinding sections. The relation between the angular position and span lengths is determined in [3].

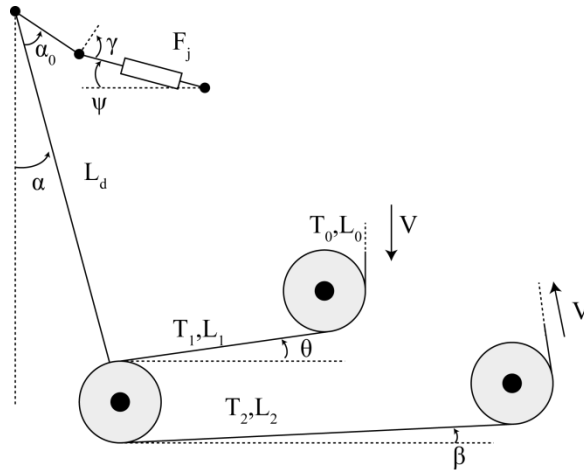


Figure 2 – Scheme of the pendulum dancer

The angular position of the pendulum dancer can be calculated by using the torque balance:

$$J_d \frac{d^2\alpha}{dt^2} = T_1(L_d - R)\cos(\alpha - \beta) + T_2(L_d + R)\cos(\alpha - \theta) - F_j L_v \cos \gamma - M_d L_{cg} \sin \alpha - C_f \quad \{4\}$$

where  $J_d$  and  $M_d$  are respectively the pendulum dancer inertia and mass;  $\alpha$  is the angular position. The web lengths and angles notations are shown in Fig. 2.  $F_j$  is the force applied by the pneumatic jack on the pendulum dancer. This force is calculated in order to achieve the expected web tension.

The web length  $L_1$  and  $L_2$  in the Fig. 2 are varying. These variations have to be taken into account in the tensions  $T_1$  and  $T_2$  calculation.

### **Linear Model**

Now, a linear model of the system can be constructed around the nominal web velocity, the nominal web tension and the nominal pendulum position. The linear tension dynamics can be expressed as follows:

$$L_i \frac{dt_i}{dt} = V_0(t_{i-1} - t_i) + (v_{i+1} - v_i)(ES + T_0) \quad \{5\}$$

where  $T_0$ ,  $V_0$  are respectively the nominal web tension and velocity.  $L_k$  is the web span length between the two rollers.  $E$  and  $S$  are respectively the web Young's modulus and the web cross-section. The Eqn. {4} can be linearized for a small angle  $\alpha$ .

$$J_d \frac{d^2\alpha}{dt^2} = T_1(L_d - R)\cos(\beta_0) + T_2(L_d + R)\cos(\theta_0) - F_j L_v \cos \gamma_0 - M_d L_{cg} \alpha - C_f \quad \{6\}$$

Then a state space model of the plant can be deduced:

$$\begin{cases} \dot{x}(t) = A(\lambda)x(t) + B(\lambda)u(t) \\ y(t) = C(\lambda)x(t) \end{cases} \quad \{7\}$$

where the matrixes  $A$ ,  $B$ ,  $C$  are depending on the uncertain parameter  $\lambda$ .

The state vector  $x$  is composed of the speed of each roller, the tension of each span, the pendulum dancer angles and theirs derivatives.

The model entry  $u$  contains the four motors torques  $u_i$ , the pneumatic jack forces  $F_1$  and  $F_2$  and the web lengths inside the two pendulum dancers.

The model output is composed of the motor velocities  $\Omega_i$ , the two pendulum dancer angles and 3 web tensions ( $T_u$  in the unwinder section,  $T_i$  in the intermediate section and  $T_r$  in the rewinder section).

$$\begin{aligned} x &= [V_1 \ T_1 \ V_2 \ \dots \ T_{29} \ V_{30} \ \alpha_1 \ \dot{\alpha}_2 \ \alpha_2 \ \dot{\alpha}_2]^t \\ u &= [u_1 \ u_2 \ u_4 \ u_4 \ L_4 \ L_5 \ F_1 \ L_{25} \ L_{26} \ F_2]^t \\ y &= [\Omega_1 \ \Omega_2 \ \Omega_3 \ \Omega_4 \ \alpha_1 \ \alpha_2 \ T_u \ T_i \ T_r]^t \end{aligned} \quad \{8\}$$

## CONTROL STRATEGY

In roll-to-roll systems two variables have to be controlled: the web speed and the web tension. To master these variables cascading control is used.

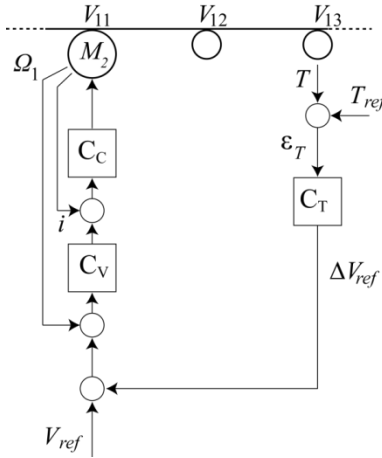


Figure 3 – Cascading control of the motor driven roller  $M_2$

Figure 3 shows the cascading control strategy used for the second driven roller  $M_2$ . The controller  $C_c$  is used to control the motor torque. This control loop is very fast and can be considered as a gain.  $C_v$  corresponds to the roller speed controller. All the motor driven rollers have the same inertia, thus the torque and speed controllers are tuned identically. Finally,  $C_T$  controls the web tension. The roller speed and web tension controllers are described more precisely in the following sections.

### Speed Control

The speed control is ensured using IP controller. The main asset of the IP controller is that it does not introduce a zero in the closed-loop transfer function [3].

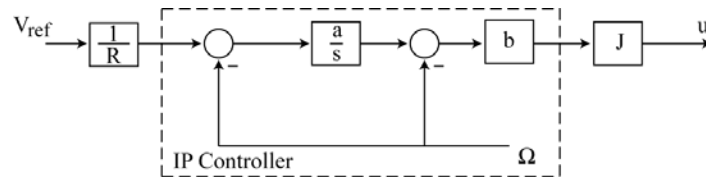


Figure 4 – IP speed controller

The speed controller scheme is given in Figure 4. The linear speed reference is divided by the roller radius in order to have a rotational speed reference. The controller output is multiplied by the roller inertia in order to simplify the speed transfer function and to be insensitive to inertia variations (for unwinder and rewinder rolls). The IP controller parameters  $a$  and  $b$  are calculated as follows:

$$a = \frac{\omega_n}{2\zeta} \quad b = \frac{\omega_n^2}{a.K} \quad \{9\}$$

where  $\omega_h$  is the desired closed loop cross-over frequency,  $\xi$  is the desired damping factor and  $K$  is the motor torque constant. In this equation, the motor friction and the torque induced by the web tension have been canceled with a feedforward approach [9].

### Tension Control

The web tension control of roll-to-roll systems is studied for several years. The system under study contains two pendulum dancer mechanisms, one in the unwinder section and the other in the rewinder section. The web tensions in these sections are imposed indirectly using pendulum dancer position control. In the intermediate section, load cells are used to control directly the web tension.

The  $H_\infty$  approach enables an automatic synthesis of the tension controllers [3][2]. The  $H_\infty$  problem consists in finding a stabilizing controller  $K$  that minimize the  $H_\infty$  norm of the transfer function between a set of exogenous inputs  $w$  and a set of performance outputs  $z$ .

$$\|T_{w \rightarrow z}\|_\infty < \gamma \quad \{10\}$$

The major drawback of the  $H_\infty$  synthesis approach is the high order of the obtained controller. Indeed, the order of the controller is equal to the sum of the system order and the weighting functions order. Using current model reduction approach, the controller order cannot always be reduced while stability and performances are preserved. In industrial applications it is highly relevant to develop design algorithms producing fixed structure and order controllers. The mathematical problem seems to be difficult to solve because fixed-order controller synthesis is formulated as a non convex problem. Recent developed algorithms or Genetic algorithms are used to optimize the  $H_\infty$  norm [3].

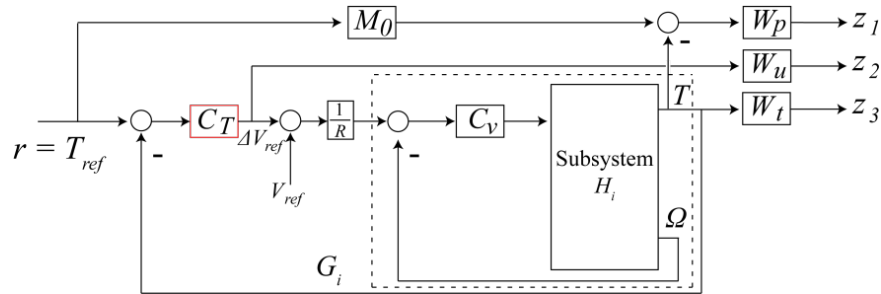


Figure 5 –  $H_\infty$  S/KS/T with model matching synthesis scheme.

The web tension controller is synthesized with output weighting functions; S/KS/T weighting scheme is given in Fig. 5. The weighting functions  $W_p$ ,  $W_u$ ,  $W_t$  appear in the closed loop transfer matrix:

$$T_{zr} := \begin{bmatrix} W_p(M_0 - T) \\ W_u KS \\ W_t T \end{bmatrix} \quad \{11\}$$

where  $M_0$  is the desired closed-loop frequency behavior.  $S$  is the sensitivity function:

$$S = (I + GK)^{-1} \quad \{12\}$$

$G$  contains the system with the speed control loops.  $K$  is the web tension controller ( $C_T/R$ ).  $T$  is the complementary sensitivity function:

$$T = I - S \quad \{13\}$$

The weighting function  $W_p$  has a high gain at low frequency in order to reject low frequency disturbances, and a desired frequency bandwidth.

The tension and the pendulum angle controllers are PI controllers in this study.

The optimization problem consists to minimize the  $H_\infty$  norm of  $T_{zr}$  with the constraints that the closed loop system has to be stable.

### INFLUENCE OF PARAMETER VARIATIONS

This study analyzes the influence of parameter variations on the global system performances (web tension and speed references tracking, tension - speed decoupling). The open-loop and closed-loop behaviors are analyzed for web elasticity, web speed and wound roll radii variations.

The frequency behavior of the open-loop system (without any controller) is studied for each parameter variations.

**Web Elasticity Variations.** Fig. 6 gives the maximum singular values of the open loop system for different Young modulus. For an increased modulus the second peaks are shifted to higher frequencies. Moreover, the second peaks gain increases with web elasticity. The peaks at low frequency correspond to the pendulum behavior.

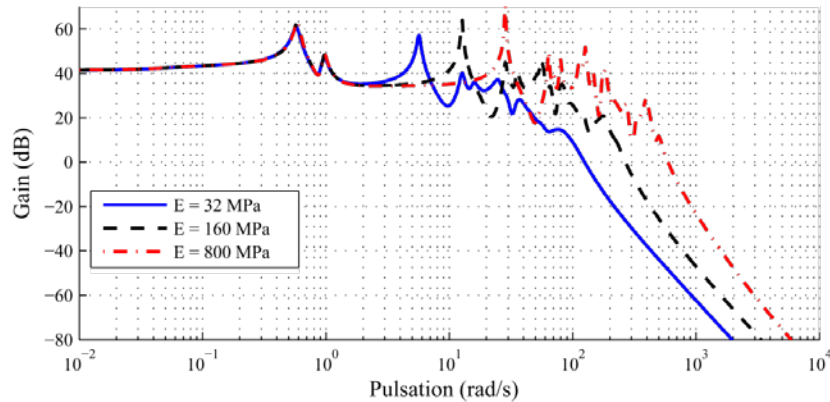


Figure 6 – Frequency behavior of the open-loop system for web elasticity variations

**Web Speed Variations.** Fig. 7 depicts the influence of web speed variations on the open-loop system. One can see that the static gain and bandwidth are unchanged. However, the resonance magnitudes (except the pendulum resonances) are reduced for a web speed rise.

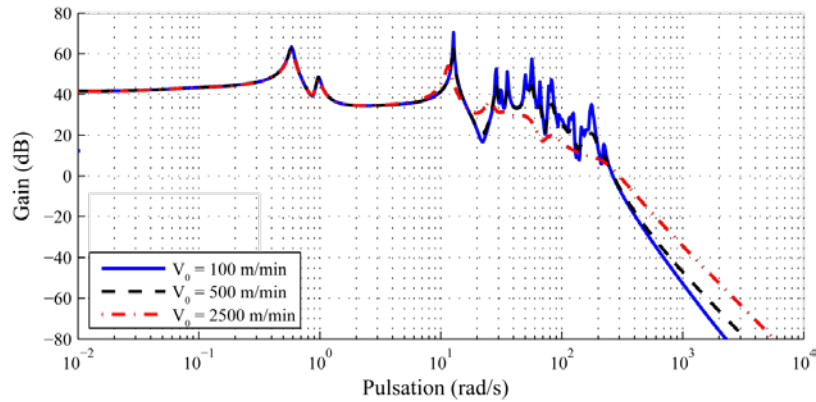


Figure 7 – Frequency behavior of the open-loop system for web speed variations

**Wound Roll Radii Variations.** One can see in Fig. 8 the effect of wound roll radii variations on the open-loop system. In the studied case, the nominal values are  $Rd = 0.5\text{m}$  (unwinder) and  $Re = 0.2\text{m}$  (rewinder). For different radii ratio essentially the static gain of the system is changed.

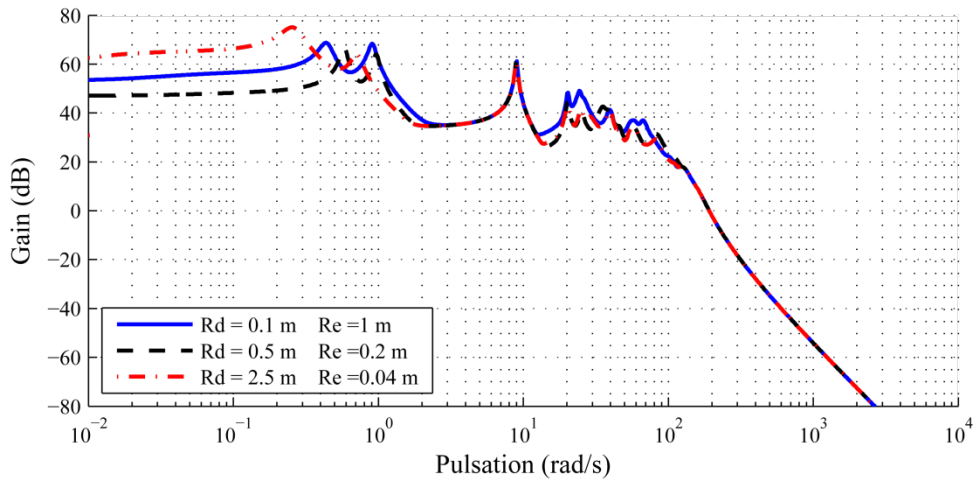


Figure 8 – Frequency behavior of the open-loop system for wound roll radii variations

### Closed-Loop Analysis

The frequency behavior of the closed-loop system (including the speed, tension and dancer angle control) is studied for each parameter variations. A time domain analysis is also made with the nonlinear model. The controllers are synthesized for the nominal values fixed as follows:

$$\begin{aligned}
 E &= 160\text{MPa} \\
 V_0 &= 500\text{ m/min} \\
 Rd &= 0.5\text{m} \quad Re = 0.2\text{m}
 \end{aligned}$$



**Web Elasticity Variations.** One can see in Fig. 9 that for an increased Young modulus the resonances are shifted to higher frequencies and their magnitudes are increased. The static gain is unchanged.

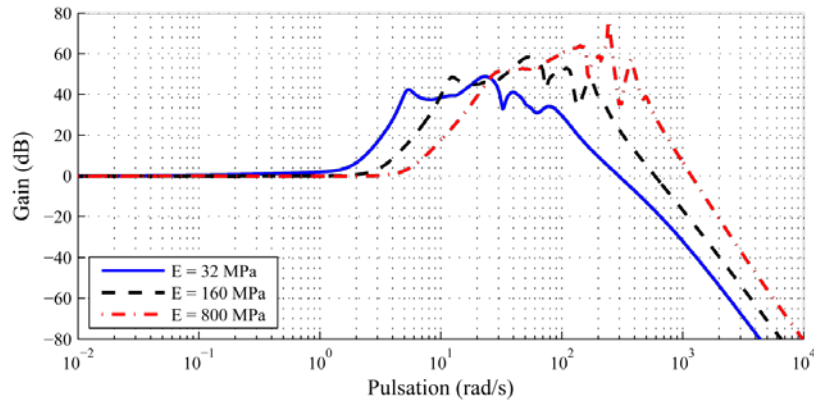


Figure 9 – Frequency behavior of the closed-loop system for web elasticity variations

Fig. 10 gives the zeros-poles map of the closed-loop. For an higher Young modulus the imaginary parts move away from the real axis whereas the real parts move to the imaginary axis. This can results to more oscillations in the time domain.

Fig. 11 shows the time domain results. One can see that a web elasticity increasing leads to high tension oscillations during the startup phase. A web elasticity decreasing has less effects on the web tension.

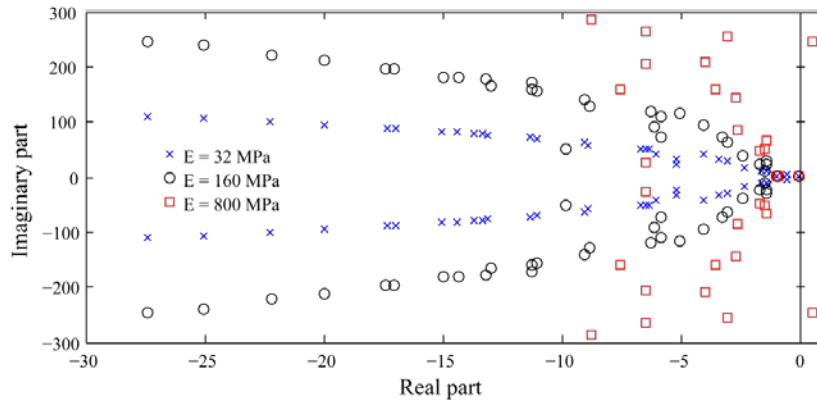


Figure 10 – Poles-zeros map of the closed-loop system for web elasticity variations

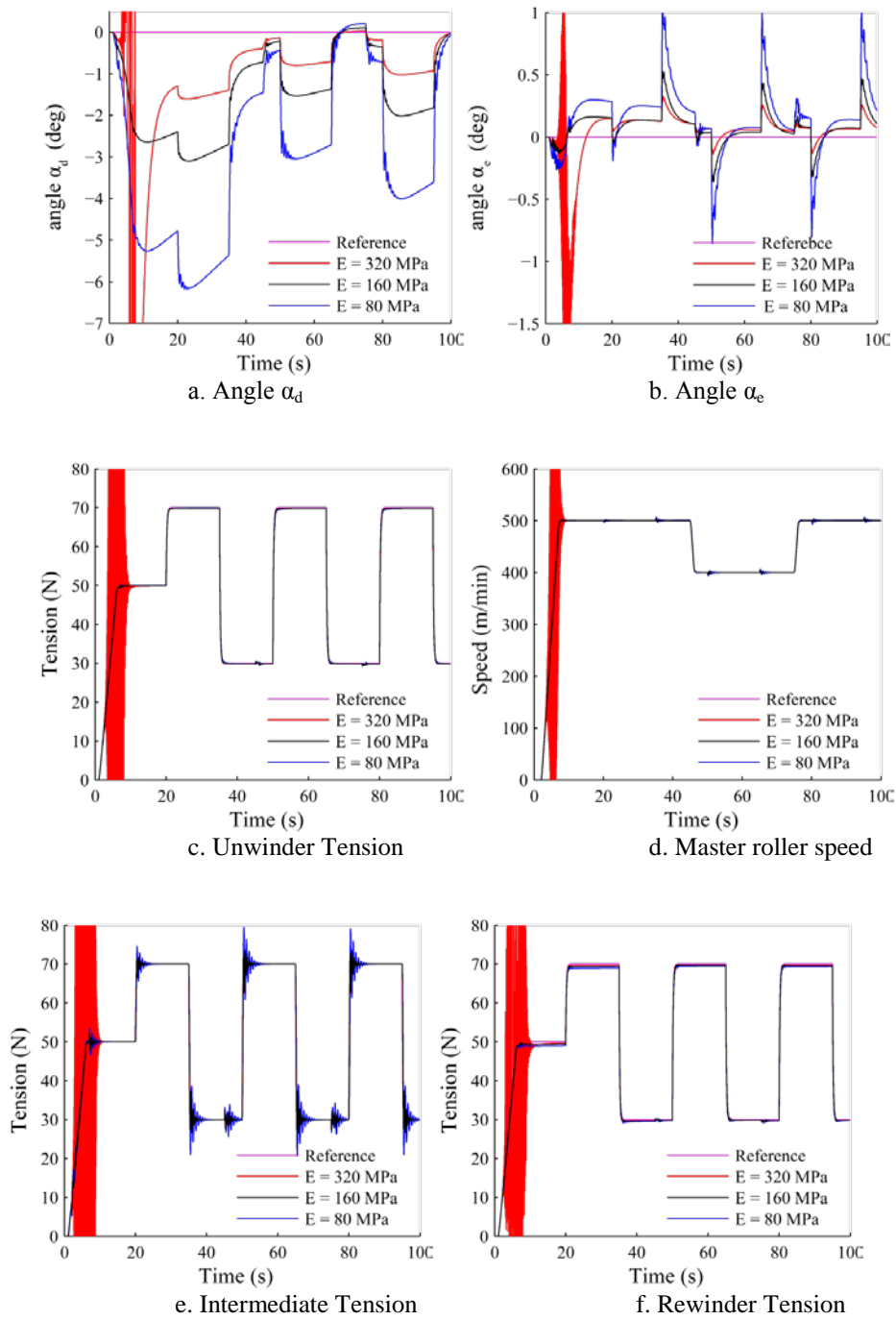


Figure 11 – Time domain results of the closed-loop system for web elasticity variations

Fig. 12 shows that the static gain and bandwidth are unchanged but the resonance magnitudes are reduced for a higher web speed. This is illustrated in Fig. 13 : the imaginary parts of the poles decrease.

Fig. 14 shows the time domain results. Good web tension behavior has been obtained for high web speed. But the pendulum dancer is more difficult to control.

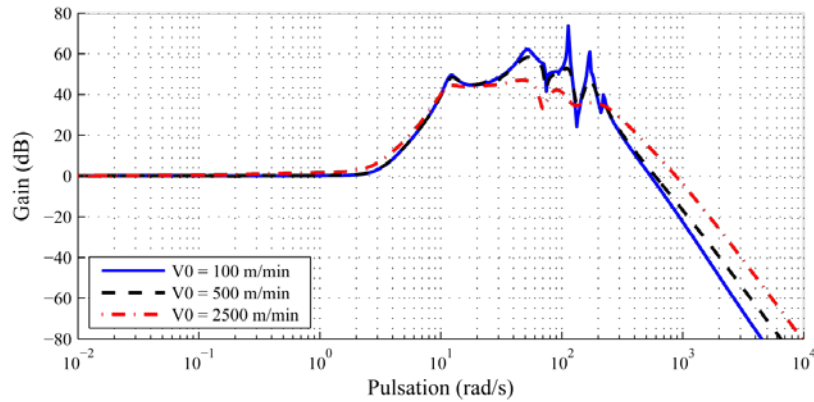


Figure 12 – Frequency behavior of the closed-loop system for web speed variations

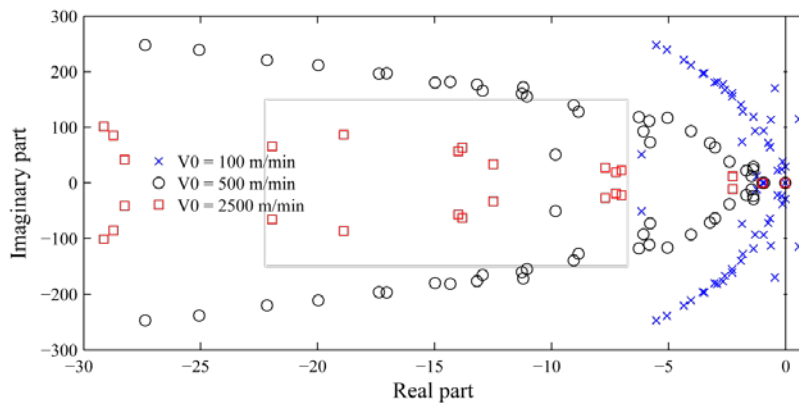


Figure 13 – Poles-zeros map of the closed-loop system for web speed variations

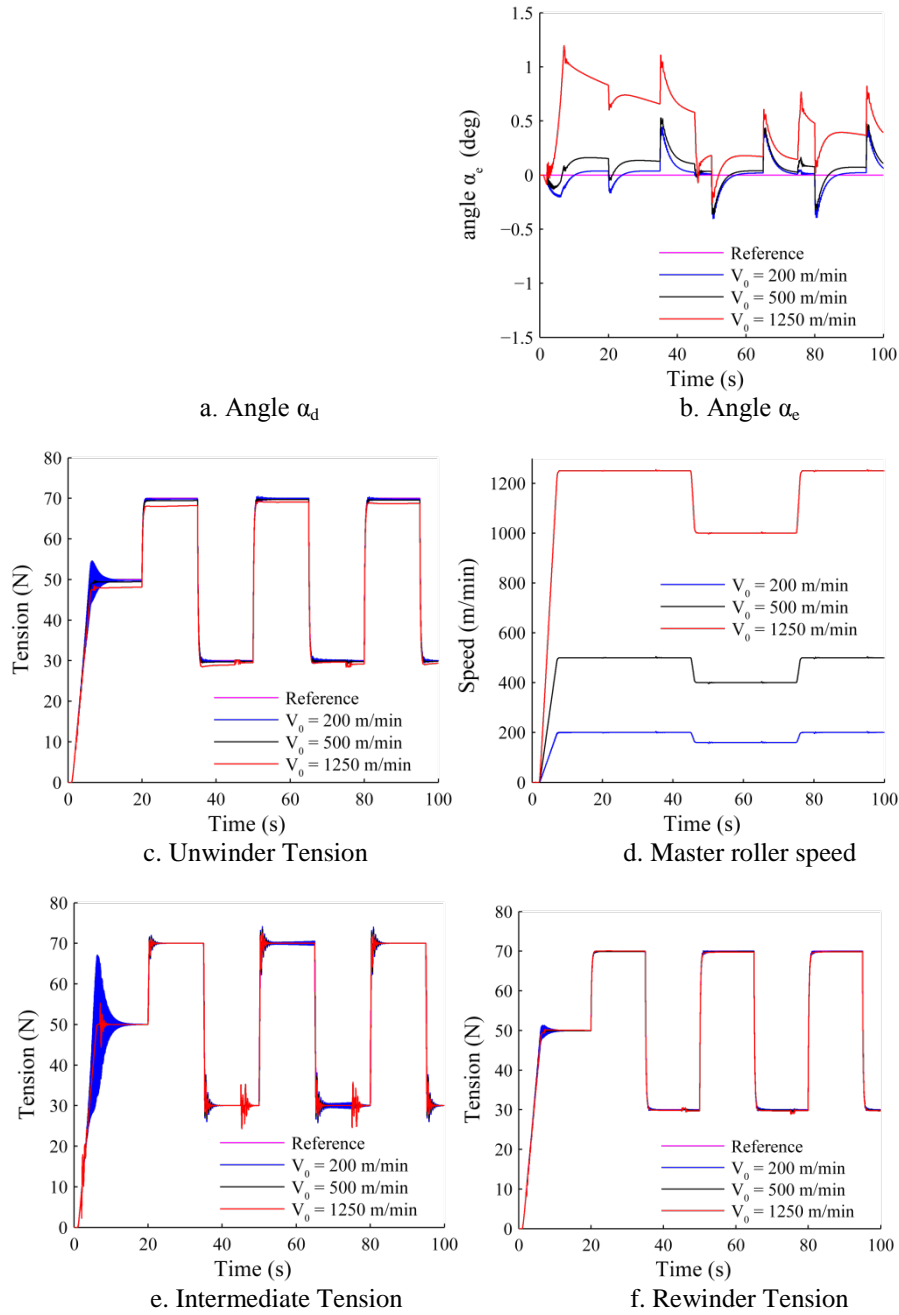


Figure 14 – Time domain results of the closed-loop system for web speed variations

**Wound Roll Radii Variations.** In this section, the online radii measurements used in the control strategy (see Fig. 5) are considered to have an error. Nevertheless, the controllers are synthesized for nominal values of the wound roll radii given in {14}, i. e. without measurement errors.

Fig. 15 to 17 highlight the effect of wound roll radii variations on the closed-loop system. For a radii ratio change the static gain varies. Nevertheless the closed-loop may become instable (see Fig. 16 : some poles are located on the right of the imaginary axis).

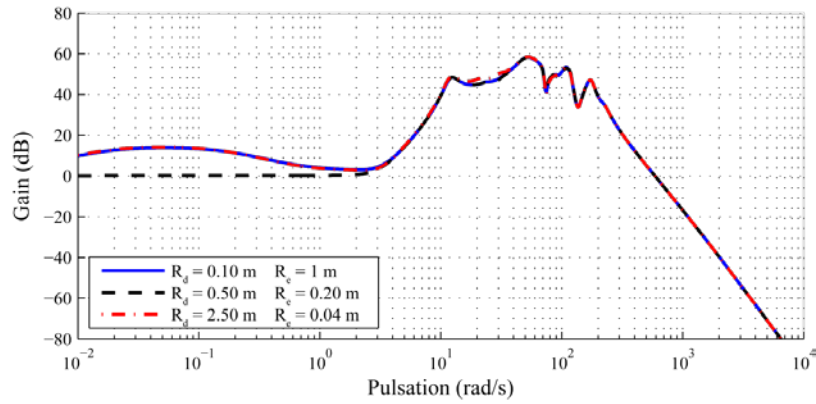


Figure 15 - Frequency behavior of the closed-loop system for wound roll radii variations

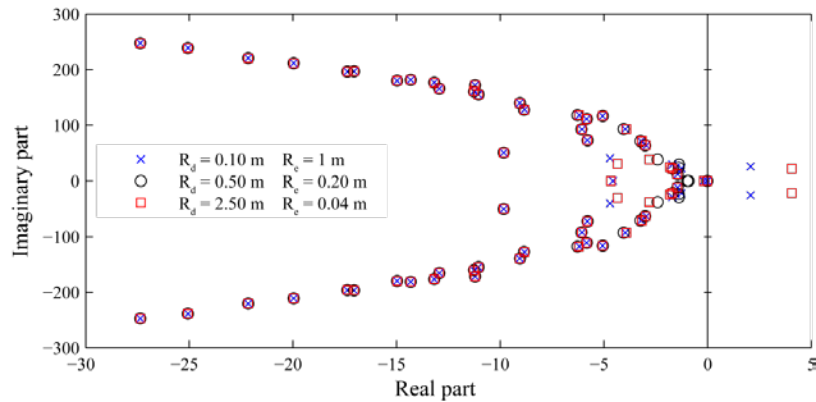


Figure 16 – Poles-zeros map of the closed-loop system for wound roll radii variations

Moreover, Fig. 17 depicts the time domain behavior of the closed-loop system subjected to a 2 per cent error on the radii measurements. Even a small measurement error has an influence on the references tracking and can lead to static errors.

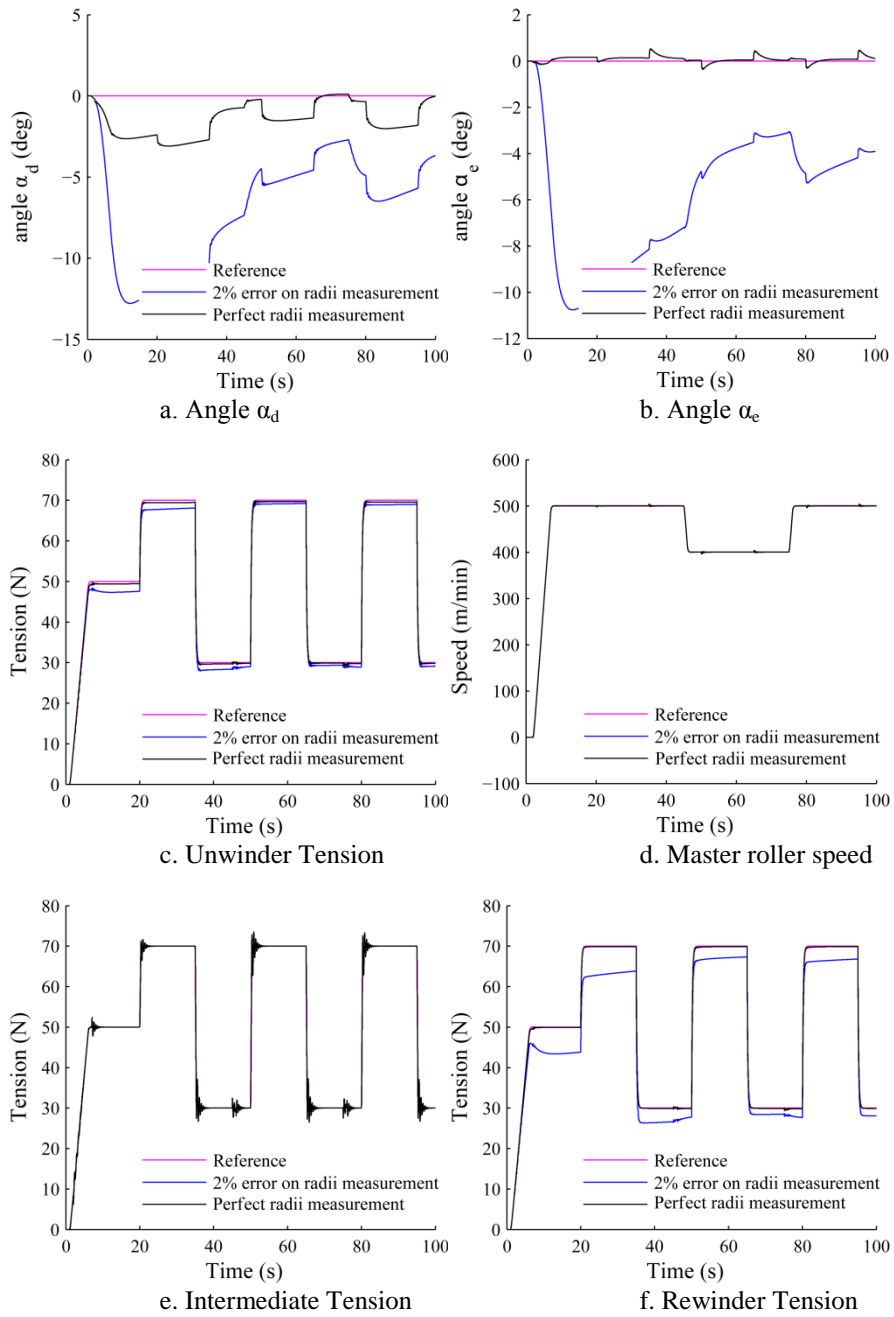


Figure 17 – Time domain results of the closed-loop system for wound roll radii measurement errors

## CONCLUSION

## REFERENCES

1. Wolfermann, W., "Tension Control of Webs. A Review of the Problems and Solutions in the Present and Future," International Conference on Web Handling, 1995, Oklahoma, pp. 198-229.
2. Koç, H., Knittel, D., de Mathelin, M., and Abba, G., "Modeling and Robust Control of Winding Systems for Elastic Webs," IEEE Transactions on Control Systems Technology, Vol. 10, No. 2, 2002, pp. 197-208.
3. Gassmann, V., "Commande Décentralisée Robuste de Systèmes D'entraînement de Bandes à Elasticité Variable," Ph.D. Thesis, University of Strasbourg, Strasbourg, France, 2011.
4. Gassmann, V., Knittel, D., Pagilla, P., and Bueno, M., "Hinf Unwinding Web Tension Control of a Strip Processing Plant Using a Pendulum Dancer," American Control Conference, St. Louis, Missouri, USA, 2009.
5. Gassmann, V., Knittel, D., Pagilla, P., and Bueno, M., "Fixed-Order Hinf Tension Control in the Unwinding Section of a Web Handling System Using a Pendulum Dancer," IEEE Transactions on Control Systems Technology, Vol. 20, No. 1, 2012, pp. 173-180.
6. Knittel, D., Laroche, E., Gigan, D., and Koç H., "Tension Control for Winding Systems with Two-Degrees-of-Freedom Hinf Controllers," IEEE Transactions on Industry Applications, Vol. 39, No. 1, 2003, pp. 113-120.
7. Kuhm, D. and Knittel, D., "New Mathematical Modeling and Simulation of an Industrial Accumulator for Elastic Webs," Applied Mathematical Modeling, Vol. 36, No. 9, 2012, pp. 4341-4355.
8. Skogestad, S. and Postlethwaite, I., "Multivariable Feedback Control: Analysis and Design," Wiley-Interscience, 2 ed., ISBN 0470011688, 2005.
9. Knittel, D., Arbogast, A., Vadrines, M., and Pagilla, P., "Decentralized Robust Control Strategies with Model Based Feedforward for Elastic Web Winding Systems," American Control Conference, 2006, pp. 1968-1975.
10. Toscano, R. and Lyonnet, P., "Robust Static Output Feedback Controller Synthesis Using Kharitonov's Theorem and Evolutionary Algorithms," Inf. Sci., Elsevier Science Inc., Vol. 180, 2010, pp. 2023-2028.
11. Benlatreche, A., Knittel, D., and Ostertag, E., "Robust Decentralized Control Strategies for Large Scale Web Handling Systems," Control Engineering Practice, 2008.
12. Gassmann, V. and Knittel, D., "Robust PI-LPV Tension Control with Elasticity Observer for Roll-to-Roll Systems," IFAC World Congress, Milan, Italy, September 2011.

13. Gassmann, V. and Knittel, D., "Hinf-Based PI-Observers for Web Tension Estimations in Industrial Unwinding-Winding Systems," IFAC World Congress, Seoul, July 2008.